Supporting information for

Droplet-assisted Fabrication of Porphyrin Colloidal Crystals from Flower-shaped Janus Particles

Ting Wang,[a] Shuoran Chen,[b] Feng Jin,[a] Jinhua Cai,[c] Liying Cui,[d] Yongmei Zheng,[b] Jingxia Wang,*[a] Yanlin Song,[b] and Lei Jiang[a,b]

1. Materials

1.1 Synthesis of 5-(4-(ethylcarboxypropoxy)phenyl)-10,15,20-tri(naphthyl) porphyrin (CPTNPP)

CPTNPP was prepared by **Scheme** S1.

HPTNPP

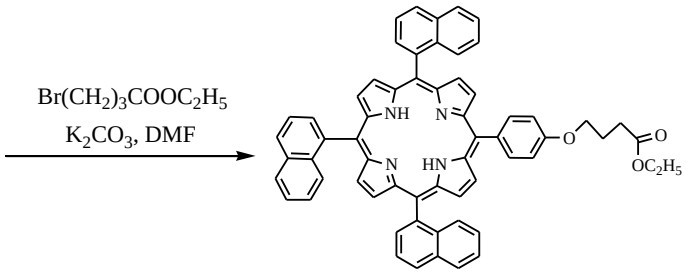

CPTNPP

Scheme S1. Synthetic procedure of CPTNPP

Firstly, HPTNPP was synthesized by the method similar to the literatures.[1] In detailed, 4.7 g naphthalaldehyde (30 mmol) and 1.2 g 4-hydroxybenzaldehyde (10 mmol) were dissolved in a mixture of acetic acid (120 ml) and nitrobenzene (60 ml). 2.7 g pyrrole (40 mmol) was added into the system followed by the temperature of system was raised to 120°C, and the system was kept at 120 °C for 1.5 h. Finally, the

solution was then allowed to cool to room temperature and purple residues were obtained by filter. The crude material was purified on a silica gel chromatograph using $CHCl_3$ as an eluent. The second band was collected and the solvent was evaporated. Purple solid HPTNPP was obtained in 2.6% yield. **ESMS** [$CHCl_3$, *m*/*z*]: 781 ($[HPTNPP]^+$). **1H NMR** (300MHz, $CDCl_3$): 8.56-8.58 (d, 8H, β-pyrroles),8.04-8.07 (d, 2H, 2,6-phenyl), 8.43-8.47(d, 6H, 2,8- naphthyl), 8.12 (s, 3H, 4- naphthyl), 7.53-7.57(d, 6H, 3,5- naphthyl), 7.45-7.49(d, 6H, 6,7- naphthyl), 7.11 (d, 2H, 3,5-phenyl), −2.36 (s, 2H, NH, pyrrole).

CPTNPP was synthesized by esterification reaction of HPTNPP. A mixture of 0.3902 g HPTNPP, 1.8 g K_2CO_3 and 50 mL N,N-Dimethylformamide(DMF) was stirred at 90 ˚C. 2mL ethyl 4-bromobutyrate dissolved in 5ml DMF was added dropwise. After 10 h, the mixture was washed with H_2O several times to neutrality, drying over anhydrous Na_2SO_4 and concentrating via rotary evaporation, the residue was chromatographed on a silica gel column using $CHCl_3$ as eluent. The first band was collected and the solvent was evaporated. Purple solid CPTNPP was obtained in 85% yield. **ESMS** [$CHCl_3$, *m*/*z*]: 895.3($[CEPTNP]^+$). **1H NMR** (300MHz, $CDCl_3$): 8.53-8.57 (d, 8H, β-pyrroles), 8.05-8.07 (d, 2H, 2,6-phenyl), 8.41-8.46(d, 6H, 2,8-naphthyl), 8.10 (s, 3H, 4- naphthyl), 7.76-7.78(d, 6H, 3,5- naphthyl), (7.41-7.47(d, 6H, 6,7-naphthyl), 7.18 (d, 2H, 3,5-phenyl), 4.16-4.26 (s, 4H, C–CH_2–O), 2.26(s, 2H, C-CH_2-C=O), (1.51 (s, 2H,C- CH_2-C), 1.29 （d, 3H, CH_3-C-）−2.39 (s, 2H, NH, pyrrole).

1.2 Fabrication of porphyrin nanostructure

1.2.1 Substrate preparation

Hydrophilic silicon wafer was obtained by being treated with a mixture of hydrogen peroxide (30%) and sulfuric acid (98%) (20:60 v/v) for 12h at 200 ℃. (Caution! Piranha solution reacts violently with organic compounds and must be handled with extreme care.) After being washed with plenty of ultrapure water (Ultrapure water was provided by a Milli-Q reference system). The silicon wafers

were blown dry with a flow of high purity argon. And the hydrophilic silicon wafers were obtained.

Hydrophobic silicon surfaces were obtained by FAs-treated of hydrophilic silicon wafer as follows: the hydrophilic silicon wafers were placed in a desiccator together with a vial containing liquid 1H, 1H2H,2H-perfluorodecyltrichlorosilane (FAS-17) (Alfa Aesar). The desiccator was evacuated, and the sample was kept in the desiccator for 12 h at 85 ℃. Finally, the sample was taken out and baked in an oven at 60 ℃ for 1 h. The water contact angles (CA) is 110.7 ° on the hydrophobic silicon wafer. The root-mean-square roughness values of the FAS-17-modified silicon surface were 1.21 ± 0.07 nm, (the standard deviation was based on five measurements).

1.2.2 Preparation of CPTNPP suspension

Porphyrin suspension is obtained by the following process: firstly, the CPTNPP is dissolved into chloroform in 10^{-5}~10^{-6} mol/L, and then the CPTNPP chloroform solution was dispersed into IPA in a changing volume ratio of IPA of 66.7%, 50%, 33.3%, 25%. And the mixture was ultrasonicated 0.5 h at room temperature to form porphyrin dispersion.

1.2.3 Fabrication of flower-shaped particles

Firstly, CPTNPP suspension was spread onto the hydrophobic cold substrate at 0℃ with the humidity of 50%. Subsequently, the water droplet template formed at the interface of air-suspension owing to the solvent evaporation, producing an new interface of water-suspension. Followed by the encapsulation of water droplet by CPTNPP vesicles and subsequent solvent evaporation, the flower-shaped Janus colloidal particles were fabricated owing to the spontaneous aggregation of the nanopetals. Interestingly, the flat side of particles is formed at the interface of air-water, while the concave side of particles is obtained at the interface of suspension -water.

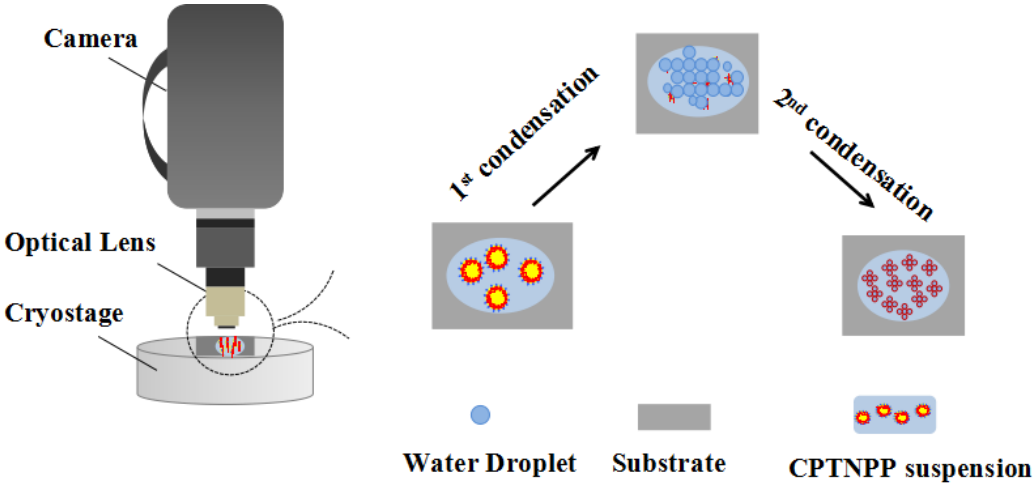

Scheme S2. The set-up diagram for the fabrication of flower-shaped particles.

This is the set-up illustration for the fabrication of flower-shaped particles. The cryostage is used to control the temperature, and the camera is used to record the *in-situ* observation of flower-shape particles.

1.3 Characterization of porphyrin nanostructures

The sizes and morphologies of porphyrin nanostructures were characterized by using scanning electron microscopy (SEM, S-4800,Japan Hitachi) operating at 5.0 kV. In order to enhance electrical conductivity, the samples were sputtered with platinum. The morphologies of samples were also characterized by using a polarized optical microscope equipped with a charge-coupled device camera (Panasonic Super Dynamic II WVCP460). AFM images were acquired using an Agilent 5500 AFM (Agilent Corp). UV-vis spectra were collected using a Hitachi U-4100. TEM image of as-prepared flower-shaped particle was obtained by JEOL, JEM 2100. Particle distribution of the CPTNPP vesicles is characterized by Malvern Lazer Particle analyzer.

1.4 The confirmation of CPTNPP vesicles in the dispersion

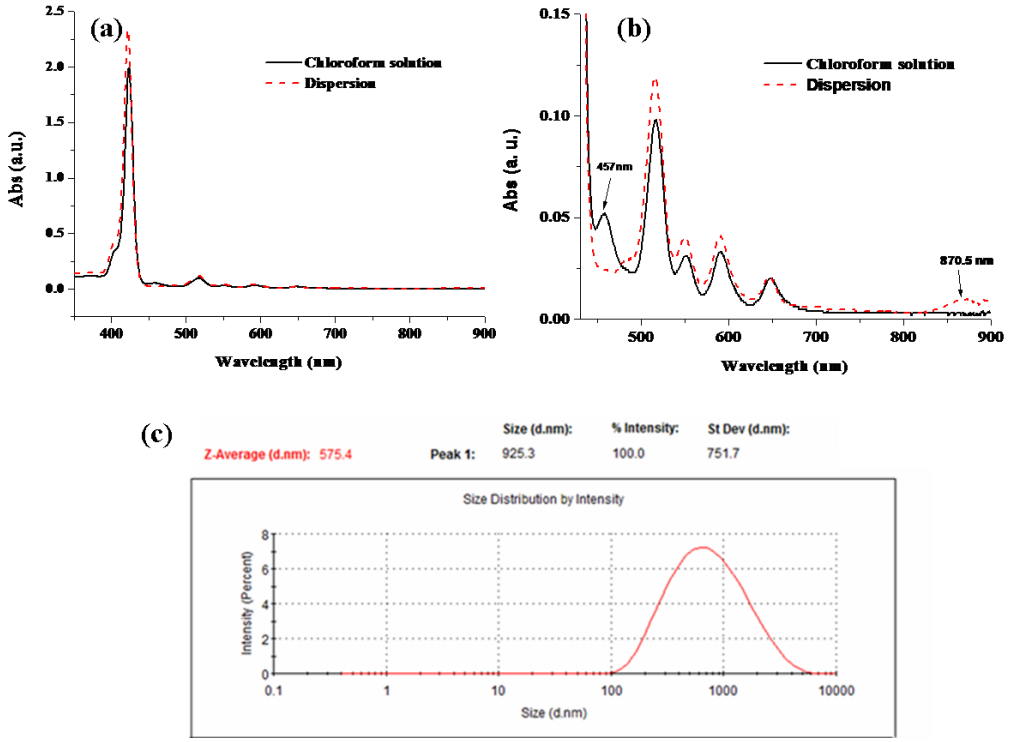

Figure S1. (a, b) UV-vis absorption spectra of the chloroform solution of CPTNPP and the CPTNPP dispersion obtained by mixing its chloroform solution and IPA at the volume ratio of 1:1. (c) Dynamic light scattering data of the CPTNPP dispersion from Malvern Lazer Particle Analyzer.

Figure S1a, b show UV-vis absorption spectra of chloroform solution of CPTNPP and the CPTNPP dispersion.

Comparing the spectra of monomeric CPTNPP in chloroform solution, the peak centered at 457.0 nm disappears, and new peak centered at 871 nm emerges for the spectra of CPTNPP dispersion. These changes indicate the difference of the CPTNPP dispersion and the chloroform solution. Indicating the possible formation of the vesicles in the CPTNPP dispersion.

The data in **Figure** S1c is obtained from dynamic light scattering of Malvern Lazer Particle analyzer for the mixing the chloroform solution of CPTNPP and IPA in

volume ratio of 1:1. It was found that the as-formed vesicle has average size of 575.4 nm, further confirming the presence of the CPTNPP vesicle in the dispersion.

1.5 Droplet formation on the experiment process

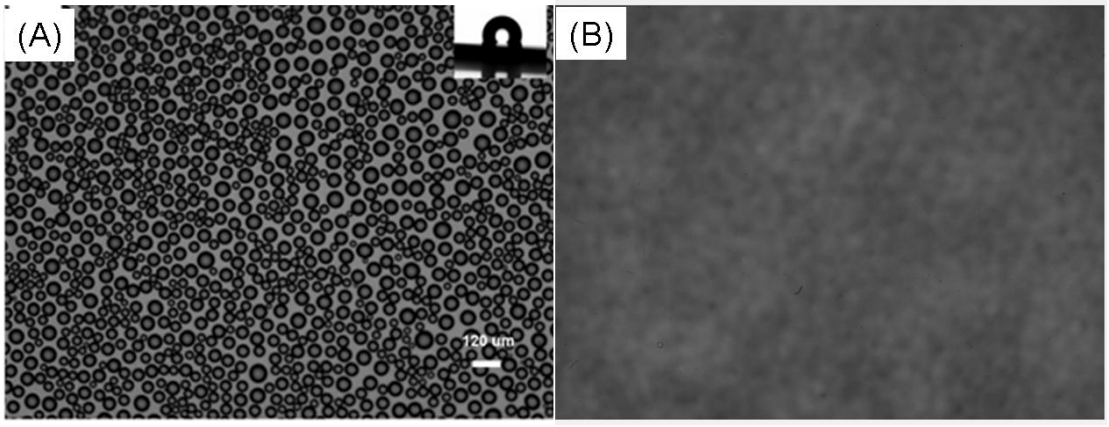

Figure S2. Droplets template formed on the (A) hydrophobic substrate and (B) CPTNPP suspension.

An obvious droplet template formed on the hydrophobic substrate (A), but the weak signal for droplet template formed on the CPTNPP suspension.

1.6 *In-situ* observation for the formation of the new interface and Janus petals.

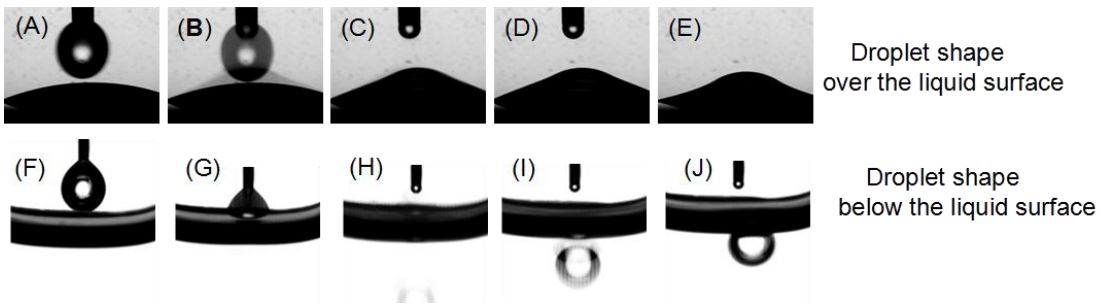

Figure S3. *in-situ* optic images for the status of droplet falling on the suspension. (A-E) demonstrate an *in-situ* observation of the droplet on the surface of the suspension (focusing on the status of the droplet over the liquid surface), resulting in a small concave one over the liquid surface as shown in (E). In contrast, (F-J) present a similar case expect focusing on the status below the liquid surface, resulting in a semi-droplet immersed in the liquid surface as shown in (J).

Accordingly, a combination of (E) and (J) depicts the status of the whole droplet. The *in-situ* images prove the presumption of the droplet status in Figure 2A.

2. Characterization of the flower-shaped particles.

2.1 TEM images for the petal particles

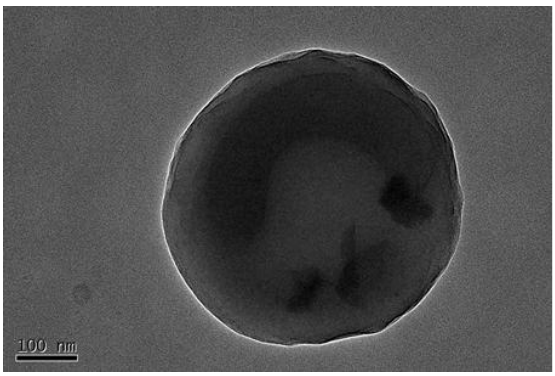

Figure S4. TEM image for as-prepared nanopetals.

It can be seen from TEM image that the hollow structure can be obtained for nanopetals.

2.2 Prediction of the petal particles by the shape of the critical water droplet

As the shape of nanopetal depends on that of droplet template, we predict the shape of the nanopetal from the droplet template by modified Yong's equation.

(1) The contact angle (CA) of the droplet on the substrate and on the suspension

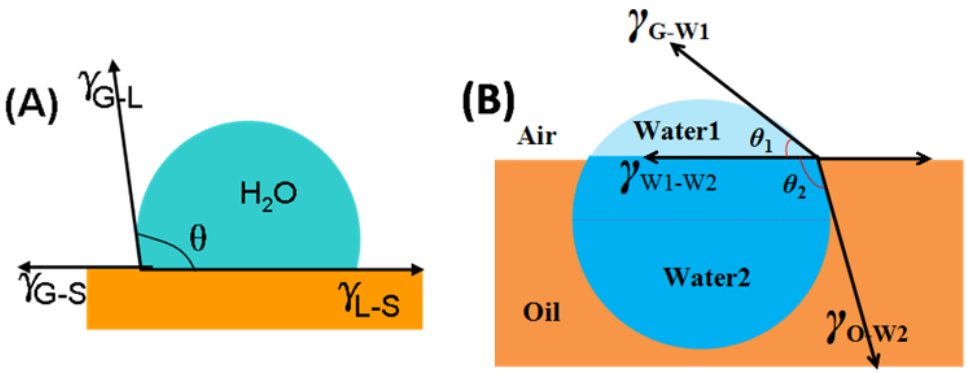

Scheme S3. The contact angle of the droplet on the (A) substrate and (B) suspension**.**

when liquid droplet sits on the substrate as shown in **Scheme 3A**, its CA (θ) can be calculated by the Young's equation (1)[1].

$$\cos\theta = \frac{\gamma_{S-G} - \gamma_{L-S}}{\gamma_{L-G}} \qquad \text{-----(S1)}$$

Wherein, $\gamma_{S\text{-}G}$ is the surface energy of the substrate, $\gamma_{L\text{-}S}$ is the surface tension of the liquid on the substrate, $\gamma_{L\text{-}G}$ is the surface tension of the water.

(2) The CA of the droplet on the suspension

When the water droplet sits on the oil suspension (mixture of the chloroform and IPA, noted by orange) as shown in **Scheme 3B**, the droplet can be separated into two parts: one part is left in the air (water 1, indicated by θ_1), while the other part is immersed into the oil (water 2, indicated by θ_2). Accordingly, the CA (θ) of the droplet can be the combination of θ_2 and θ_1, that can be calculated by the modified Young's equation.

For triphase of air-W1-oil, $\cos\theta_1 = \frac{\gamma_{O-G} - \gamma_{W1-W2}}{\gamma_{W1-G}}$ ----------(S2)

For triphase of air-W2-oil, $\cos\theta_2 = \frac{\gamma_{W1-W2} - \gamma_{O-G}}{\gamma_{O-W2}}$ ----------(S3)

$\gamma_{G\text{-}W1}$ means the surface tension of water1 in air, $\gamma_{G\text{-}O}$ is the surface tension of the oil in air, $\gamma_{G\text{-}W2}$ is the surface tension of the water2 in air, $\gamma_{W1\text{-}W2}$ is the interfacial tension of the w1 and w2. $\gamma_{O\text{-}W2}$ is the interface tension of the oil and W2.

Accordingly, $\frac{\cos\theta_1}{\cos\theta_2} = -\frac{\gamma_{O-W2}}{\gamma_{W1-G}}$ ----------(S4)

Presuming w1=w2, $\frac{\cos\theta_1}{\cos\theta_2} = \frac{\gamma_{O-W2}}{72}$ ----------(S5)

(3) The shape of the Janus nanopetal

Because the nanopetal is obtained by taking the droplet as template(in Scheme S3B), the nanopetals is a combination of the two parts. The top one is determined by

θ_1, while the below one is determined by θ_2. $\frac{\cos\theta_1}{\cos\theta_2} = \frac{\gamma_{O-W_2}}{72}$ indicating the resultant shape of the nanopetal is determined from the interface tension between water and oil phase.

Table S1 presents the interface tension of water phase (water mixing with IPA in a different fraction) and oil phase (chloroform mixing of IPA in a different fraction). It can be found the Maximum interface tension is 29.49, and the value lowers with increasing fraction of IPA in either oil or water phase. Thus ,the value of $\cos\theta_1/\cos\theta_2$ is lower than 0.4, predicting the resultant particles is an uneven shape.

Table S1. The interfacial tension between water phase and oil phase

Oil phase: the fraction of IPA in chloroform (vol%) \ Aqueous phase: the fraction of IPA in the water dropelt (vol%)	0	2	4	6	8	10	15	20	30
0	29.49	25.83	21.75	18.83	16.32	14.51	10.83	8.09	4.64
2	24.23	21.64	19.91	17.83	15.51	13.69	10.26	7.33	4.38
6	23.33	19.13	17.27	13.21	12.68	12.85	9.50	7.16	4.24
10	17.84	15.61	14.03	10.68	10.6	10.03	8.66	6.54	3.64
15	16.69	13.39	11.99	8.82	8.5	8.29	7.41	5.88	3.56
20	11.91	8.56	7.91	7.02	6.79	6.81	6.29	5.39	3.26

2.3 *In-situ* observation of the formation process of flower-shaped particles.

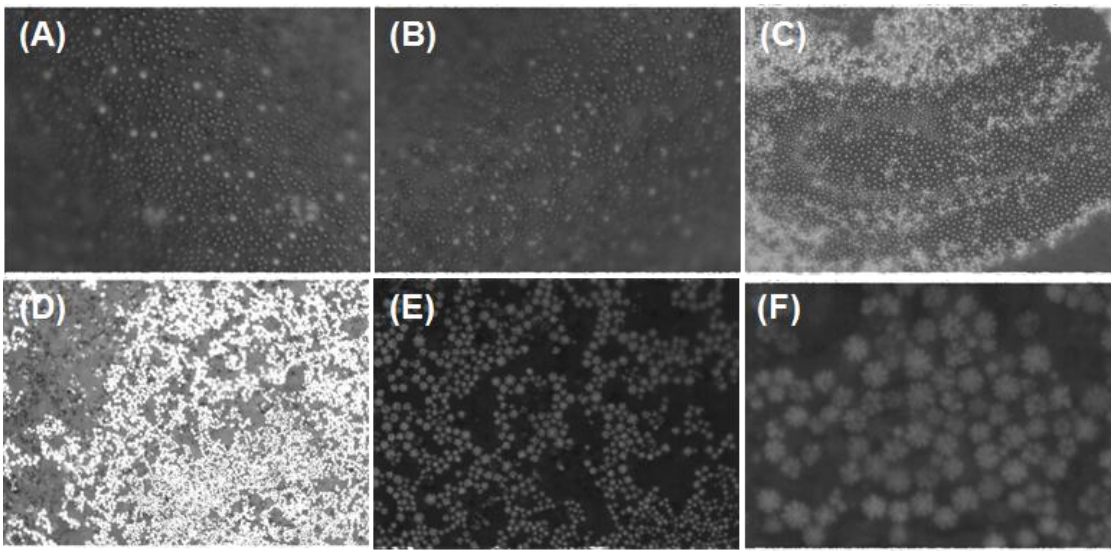

Figure S5. *In situ o*ptical images for the formation process of flower-shaped particles with prolonging grow time after 2nd water condensation process.

Figure S5 presents *in situ* optic images for the formation process of flower-shaped particles with increasing growing time. At first, no obvious image is observed for the water droplet template forming at the suspension (A, B). Subsequently, some shinning point occur to the surface after exposing the system onto 2nd water condensation(C). Furthermore, the shinning part grows with prolonging exposing time(D). When taking a close at the shinning part, beautiful flower-shaped particles can be observed (E,F).

2.4 Various flower-shaped particles

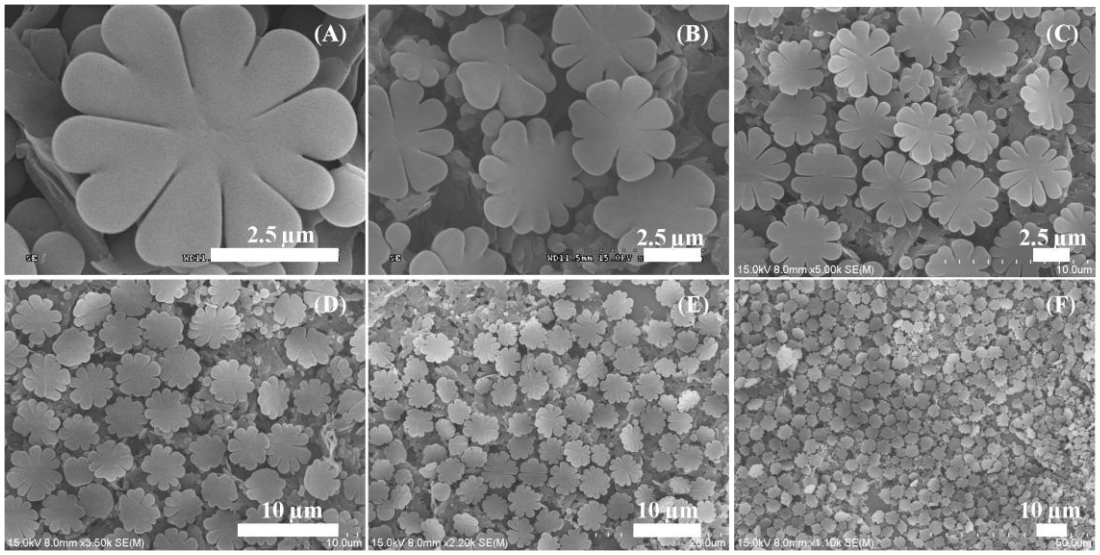

Figure S6. SEM images with different magnification for flower-shaped particles

Clearly, large area flower-shaped particles have been formed, spanned more than hundreds of micrometer. Moreover, there is a consistent orientated arrangement for the flower-shaped particles, with its flat back-side toward the air, and the concave front -side toward the substrate.

It can be found that the diameter of the flower-shaped particles are *ca.* 4~6 μm. And height of flower is *ca.* 1.5~2.5 μm in multi-layer flower and *ca.* 0.8~1.5 m in one-layer flower. The diameter of the petal is *ca.* 700 nm~1 μm, and the height of petal particles is *ca.* 0.5~0.8 μm.

3. Optical properties of porphyrin colloidal crystals from flower-shaped particles

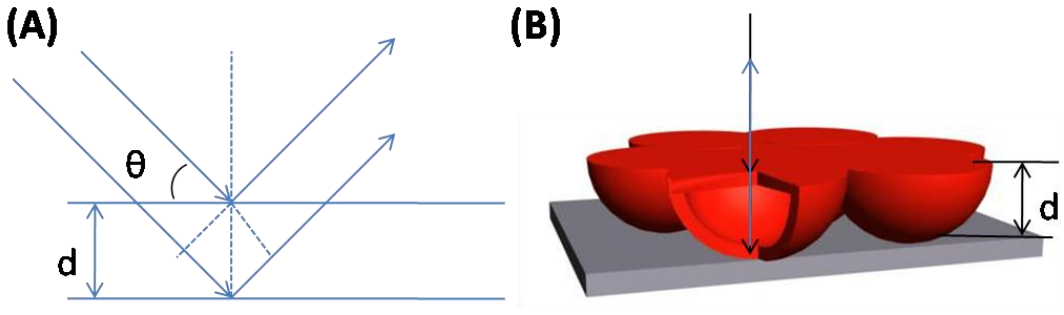

Scheme S4. The scheme of Reflection spectrum produced from flower-shaped particles

Owing to the consistent arrangement of the flower-shaped particles, the optic properties of the colloidal crystals can be explained by the transformed Bragg equation[2-4] as following:

$$\lambda_{max} = 2dn_{eff} \sin\theta \quad \text{----------} \quad \text{(S6)}$$

Where λ_{max} is the wavelength of the diffraction peak; n_{eff} is the effective refractive index of the hollow CPTNPP flower-shaped particles; d is the thickness of the building blocks in large area of flower-shaped particles, in our case, d_{petal} = 0.5~0.8 μm, $d_{one\text{-}layer\ flower}$ = 0.8~1.5 μm, $d_{multi\text{-}layer\ flower}$ = 1.5~2.5 μm; θ is an incidence angle of testing light, and θ = 90 °in our experiment;

n_{eff} is given by Eq. (5):

$$n_{eff} = \left[n_{flower}^2 f + n_{air}^2 (1-f) \right]^{1/2} \quad \text{----------} \quad \text{(S7)}$$

where n_{flower} and n_{air} are the refractive index of flower-shaped particles and air, respectively; f is the filling ratio of the hollow CPTNPP flower-shaped particles (f = 0.74);

For the flower-shaped particles, n_{flower} can be calculated by Eq. (6):

$$n_{flower} = \frac{n_{CPTNPP} V_{CPTNPP}}{V} + \frac{n_{air} V_{air}}{V} \quad \text{----------} \quad \text{(S8)}$$

where n_{CPTNPP} and n_{air} are the refractive index of CPTNPP and air respectively; V_{CPTNPP} and V_{air} are the volumes of CPTNPP and air in the hollow flower-shaped particles respectively; V is the total volume of each component ($V = V_{CPTNPP} + V_{air}$).

We assumed that n_{CPTNPP}=1.6, n_{air}=1.00 and V_{CPTNPP}= V_{air}=*1/2V*, the calculated n_{eff}= 1.229,

$$\lambda_{max} = 2.45 \text{----------} \quad \text{(S9)}$$

It can be observed from SEM images in Figure S2 that there are three kinds of thickness for building blocks of petals, one-layer flower particles, multi-layer flower particles, such as*:* d_{petal} = 0.5~0.8 μm, $d_{one\text{-}layer\ flower}$ = 0.8~1.5 μm, $d_{multi\text{-}layer\ flower}$ =1.5~2.5 μm. It can be calculated from equation S7 that λ_{max} = 1.9, 3.6 and 6.1 μm. Accordingly, there is a good agreement between the calculated and measured results

as shown in Table S1.

Above all, the optic properties can be modulated by varying the experimental conditions.

Table S2. Comparison of calculated and the measured *λmax* for the as-prepared flower-shaped assembly based on the three different building blocks.

	λ_{max} from petal	λ_{max} from single-layer	λ_{max} from multi-layer flower
Measured	2 (*d*=0.5~0.8 μm)	3.6 (*d*=0.8~1.5 μm)	5.5 (*d*=1.5~2.5 μm)
Calculated	1.9	3.6	6.1

4. The aggregate mode of CPTNPP in flower-shaped particles

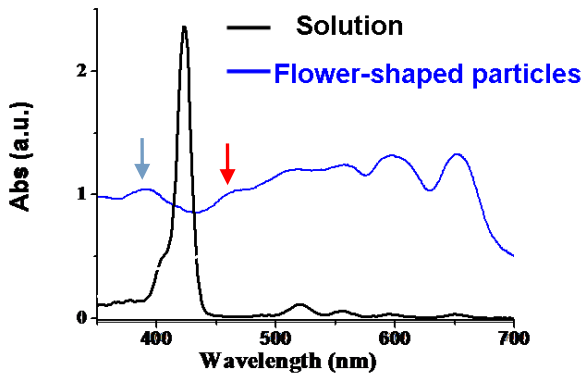

Figure S7. UV-vis absorbance spectra of CPTNPP solution and the film assembled from flower-shaped particles.

Compared to the Soret-band of the monomeric CPTNPP dispersed in chloroform (centered at *ca.* 420 nm), the flower-shaped assemblies display a split blue-shifted Soret-band at *ca.* 391 nm and part red-shifted Soret-band at 464 nm (the peak is noted by arrows), suggesting that most of the CPTNPPs therein are possibly organized as J-like aggregates.

References:

[1] a) T. Yang, *Philos. Trans. R. Soc*. London, 1805, *95*, 65; b) M. Liu, Z. Xue, H. Liu, L. Jiang, *Angew. Chem. Int. Ed.*, 2012, *51*, 8348.

[2] Y. Huang, J. M. Zhou, B. Su, L. Shi, J. X. Wang, S. R. Chen, L. B. Wang, J. Zi, Y. L. Song, L. Jiang. *J. Am. Chem. Soc.* 2012, *134*, 17053.

[3] Q. S. Jiang, K. Li, H. L. Wei, L. Yi, *J. Sol-Gel Sci. Technol.*, 2013, *67*, 565.

[4] L. Xu, H. Li, X. Jiang, J. X. Wang, L. Li, Y. L. Song, L. Jiang, *Macromol. Rapid Commun.,* 2010, *31*, 1422